Available online at BCREC website: https://bcrec.id

Bulletin of Chemical Reaction Engineering & Catalysis, 15 (3) 2020, 885-897

Research Article

Syngas Production *via* Methane Dry Reforming over La-Ni-Co and La-Ni-Cu Catalysts with Spinel and Perovskite Structures

Hassiba Messaoudi[1,4,*], Sébastien Thomas[2], Samira Slyemi[1], Abdelhamid Djaidja[1,3], Akila Barama[1]

[1]*Laboratoire des Matériaux Catalytiques et Catalyse en Chimie Organique, Faculté de Chimie, Université des Sciences et de la Technologie Houari Boumediene, BP 32 El Alia, 16111Bab Ezzouar, Alger, Algeria.*
[2]*Institut de Chimie et Procédés pour l'Énergie, l'Environnement et la Santé, UMR 7515 CNRS-Université de Strasbourg, Groupe "Énergies et Carburants pour un Environnement durable", 25 rue Becquerel, 67087 Strasbourg Cedex 2, France.*
[3]*Laboratoire des Procédés pour Matériaux, Energie, Eau et Environnement, Faculté des Sciences et des Sciences Appliquées, Université de Bouira, rue Drissi Yahia, 10000 Bouira, Algeria.*
[4]*Faculté des Sciences, Département Sciences de la Matière, Université d'Alger 1, 2 Rue Didouche Mourad, Alger centre 16000, Alger, Algeria.*

Received: 1st November 2020; Revised: 18th December 2020; Accepted: 19th December 2020; Available online: 26th December 2020; Published regularly: December 2020

Abstract

In this paper, the catalytic properties of La-Ni-M (M = Co, Cu) based materials in dry reforming of methane (DRM) for syngas (CO + H_2) production, were studied in the temperature range 773−1073 K. The $LaNi_{0.9}M_{0.1}O_3$ and $La_2Ni_{0.9}M_{0.1}O_4$ (M = Co, Cu and Ni/M = 0.9/0.1) catalysts were prepared by partial substitution of Ni by Co or Cu using sol-gel method then characterized by XRD, H_2-TPR and N_2 physisorption. The XRD analysis of fresh catalysts showed, in the case of Co-substitution, the formation of La-Ni and La-Co perovskite and spinel structures, while only $LaNiO_3$ and La_2NiO_4 phases were observed for the Cu-substituted samples. The substitution of these two structures by copper decreases the reduction temperature compared to cobalt. The reactivity results showed that the partial substitution of nickel by copper decreases the methane activation temperature, whereas a better stability of catalytic activity and syngas production was obtained via the cobalt-substituted catalysts, which is due to a synergistic effect between Ni and Co. The TPO analysis carried out on the spent catalysts indicated that the lowest carbon deposition was obtained for the cobalt substituted samples.

Keywords: Perovskite; Spinel; Transition metals; Dry reforming; Syngas

How to Cite: Messaoudi, H., Thomas, S., Slyemi, S., Djaidja, A., Barama, A. (2020). Syngas Production *via* Methane Dry Reforming over La-Ni-Co and La-Ni-Cu Catalysts with Spinel and Perovskite Structures. *Bulletin of Chemical Reaction Engineering & Catalysis*, 15(3), 885-897 (doi:10.9767/bcrec.15.3.9295.885-897)

Permalink/DOI: https://doi.org/10.9767/bcrec.15.3.9295.885-897

1. Introduction

Syngas (H_2+CO) is an essential raw material for several reactions in the petrochemical industry, especially for the production of higher hydrocarbons [1]. The syngas is principally provided via the methane reforming through one of the three processes [2−4], i.e. steam reforming, partial oxidation and dry reforming by CO_2. Among these processes, the dry reforming of methane (DRM) is considered the most promis-

* Corresponding Author.
Email: messaoudihassiba@gmail.com (H. Messaoudi);

ing reaction since it allows at the same time the conversion of methane into synthesis gas (with an equimolar ratio H_2/CO) by using CO_2 (greenhouse gas) which also contributes to the reduction of this gas emissions in the environment [5].

$CH_4 + CO_2 \leftrightarrow 2CO + 2H_2$ $\Delta H^\circ_{298\,K}$=+247 kJ/mol

The DRM process requires high energy because it is a highly endothermic reversible reaction [6]. Indeed, a very high temperature is necessary for the course of the reaction and the formation of synthesis gas as the main product of this reaction [7]. In this case, the purpose of using catalysts is to reduce the energy required to obtain a high yield of syngas.

However, like all the other catalytic processes which are carried out at high temperature, the DRM reaction is also confronted with problems of catalysts deactivation due to sintering and carbon deposition phenomena [8]. In fact, these problems cannot be completely avoided because they are linked to thermodynamics at high temperatures at which the reaction is performed. Whereas, these phenomena can be limited by bringing about changes in the operating conditions of the reaction or even on the structure and properties of the used catalysts [9].

Diverse catalytic systems are used in the DRM reaction in particular nickel supported catalysts [10] because of their high efficiency and low cost compared to noble metal catalysts [11]. Otherwise, the use of well-defined structures in methane reforming reactions is getting a lot of attention and is currently considered as one of the interesting alternative materials to minimize the problems of sintering and rapid deactivation of catalysts encountered with conventional supported nickel-based systems [12−14]. Indeed, the insertion of the nickel into a defined structure like spinel and perovskite has several advantages such as a well dispersion of nickel particles, a strong interaction that makes the nickel species less mobile than on the surface of a conventional support and furthermore a favored regeneration of nickel metallic sites by an in situ reduction. These properties should therefore improve the catalytic activity and stability of nickel species by limiting the formation of large aggregates and consequently reducing the coke deposition. Guo *et al.* [15] found that the $Ni/MgO\text{-}\gamma Al_2O_3$ and $Ni/MgAl_2O_4$ catalysts tested in the dry reforming of methane exhibit better stability and higher activity compared to $Ni/\gamma Al_2O_3$ system. In the one hand, these good catalytic performances were attributed to the formation of $MgAl_2O_4$ spinel in $Ni/MgO\text{-}\gamma Al_2O_3$, which stabilizes small Ni crystallites. On the other hand, the high activity of the $Ni/MgAl_2O_4$ catalyst compared to $Ni/\gamma Al_2O_3$ were mainly related to the characteristics of the $MgAl_2O_4$ spinel support, that reduces the sintering phenomena of nickel active phase. In addition, according to these authors, the formation of $NiAl_2O_4$ is completely avoided over $MgAl_2O_4$ spinel phase and that strong interactions between nickel and $MgAl_2O_4$ produce highly dispersed active Ni species leading to high catalytic reactivity [15].

Other studies reported that La and Ni spinel and perovskite structures were found to be very interesting catalysts in the DRM reaction because of the uniform dispersion of Ni thus reducing Ni^0 segregation and the generated La_2O_3 that interact with CO_2 to form $La_2O_2CO_3$ intermediates, which help to decrease coke formation [16−18]. Furthermore, it has been confirmed in our previous work, that the use of $MgAl_2O_4$ spinel as catalytic support for the $LaNiO_3$ and La_2NiO_4 catalysts increases the CH_4 and CO_2 conversions and enhanced the catalytic stability [3].

In order to further improve the catalytic activity and the metal dispersion, the effect of nickel doping with another transition metal has also been the subject of many studies. Indeed, these bimetallic systems have exhibited very good catalytic performances [19−21] due to the synergistic effect between the nickel and the inserted metal, which contributes to the improvement of the activity and stability of the final catalyst. In a study on bimetallic catalysts, Fan *et al.* [22] compared the conversion rates of methane on $Ni/MgO\text{-}ZrO_2$, $Co/MgO\text{-}ZrO_2$, and $Ni\text{-}Co/MgO\text{-}ZrO_2$ catalysts. Bimetallic Ni-Co reached 80% methane conversion at 1023 K, higher than those observed with monometallic catalysts Ni and Co (70% and 71%, respectively). The increase of the catalytic activity of the bimetallic compound relative to the monometallic ones has been synonymous with the synergistic effect due to the coexistence of small particles of both Ni and the added metal. Another work developed by Nataj *et al.* [23] studied the effects of nickel and copper loadings and reaction temperature on the reactivity of $Ni\text{-}Cu/Al_2O_3$ catalysts in methane dry reforming. The results indicated that the catalytic activity was strongly influenced by the amounts of Cu. Furthermore, sintering of active phases during the reaction was restricted by the formation of Ni-Cu alloy that leads to the improvement of both catalyst activity and stability. However, the promoting effects of copper were significantly faded by increasing

Cu content. Samples with high amounts of copper presented lower activity and rapid deactivation due to the agglomeration of active phase and Ni covering.

In this context, the present work is focused on the study of the catalytic performances of Ni-M bimetallic materials (M = Co, Cu) of well-defined perovskite and spinel structures in the methane dry methane reaction for the production of synthesis gas. The bimetallic catalysts were prepared by the substitution of 10 mol% of Ni by cobalt or copper in the monometallic structure $LaNiO_3$ and La_2NiO_4.

2. Materials and Methods

2.1 Catalysts Preparation

Non substituted La-Ni and substituted La-Ni-M (M = Co, Cu) with spinel and perovskite structures were prepared by the sol-gel method using nitrates salts and citric acid as raw materials [24]. The non substituted samples are perovskite $LaNiO_3$ (noted LN3) and spinel La_2NiO_4 (noted LN4). While the nickel substituted solids by copper or cobalt are perovskite $LaNi_{0.9}M_{0.1}O_3$ (noted LNM3) and spinel $La_2Ni_{0.9}M_{0.1}O_4$ (noted LNM4) with M = Co, Cu. The corresponding loadings for Co and Cu, respectively are 2.4 wt% and 2.5 wt% in the LNM3 samples and 1.5 wt% and 1.6 wt% in the LNM4 solids.

The preparation consists of dissolving the nitrate salts $La(NO_3)_3.6H_2O$, and $Z(NO_3)_2.6H_2O$ (Z = Ni, Co, Cu) in 10 mL of deionized water, according to the stoichiometric ratios of perovskite and spinel structures. The citric acid is then added with a molar ratio of citrate to metallic ions equal to 3.0. The resulting solution is left under stirring and heating at 353 K until a green gel is obtained which is dried at 393 K for 12 hours. The final precursors were calcined at 1023 K (5 $K.min^{-1}$) for 6 hours in the case of the perovskite and 4 hours for the spinel. The calcination conditions were fixed after several tests of heat treatments during different times and at various temperatures in order to obtain high crystallinity under moderately severe conditions.

2.2 Catalysts Characterization

2.2.1 Powder X-Ray diffraction (XRD)

The structure of the fresh, reduced and used catalysts was studied by the X-Ray diffraction analysis using a Bruker AXS-D8 diffractometer with a Cu-Kα radiation (λ=1.5406 Å). The XRD patterns were recorded in a 2θ range of 10-80° with a step size of 0.020° and a time of 0.80 s per step. The phase composition was determined using powder files (PDF-ICDD).

2.2.2 Surface area measurements (BET)

The specific surface areas of the different samples were obtained by measuring nitrogen adsorption-desorption isotherms at 77 K using a Micromeritics ASAP 2420 instrument. Prior to measurements, around 100 mg of sample were outgassed under vacuum at 523 K for 12 h. The BET surface areas were calculated with the Brunauer, Emmett and Teller model in the range of P/P_0 of 0.05-0.30. The pore size distribution was determined using the Barrett-Joyner-Halenda (BJH) method.

2.2.3 Temperature programmed reduction (H_2-TPR)

The reducibility of the catalysts was studied by the temperature programmed reduction (H_2-TPR) on a Micromeritics Auto ChemII 2920 apparatus. The catalyst (around 50 mg) was heated from room temperature to 1173 K (10 $K.min^{-1}$) under a flow of 10% H_2 in argon (50 $mL_{SATP}.min^{-1}$). The reduction temperatures, the H_2-consumption as well as the reduction degree (called '% red') of the different samples were measured by this technique. The % red designates the ratio between the number of moles of experimental and theoretical H_2 consumed by the sample.

2.2.4 Temperature programmed oxidation (TPO)

The analysis of the carbon deposits on the surface of spent samples (after catalytic test in DRM) was carried out by TPO analysis coupled to a mass spectrometer with a Pfeiffer Vacuum instrument QMS 2000 Prisma. Around 10 mg of used sample were subjected to a flow of helium (15.0 $mL_{SATP}.min^{-1}$) from room temperature to 1073 K (15 $K.min^{-1}$) to desorb the carbonates. After cooling to 323 K, the TPO was carried out under 1.0% mol O_2 in He (15.0 $mL_{SATP}.min^{-1}$) up to 1073 K with a temperature ramp of 8 $K.min^{-1}$.

2.3 Catalytic reaction

Catalytic tests in methane dry reforming using a molar ratio CH_4/CO_2 = 1.0 (Figure 1) were conducted at atmospheric pressure using a quartz reactor in form I (length 300 mm, inner diameter 7.0 mm) placed in an experimental setup previously described [4], in the temperature range 773−1073 K. The catalyst (15.0 mg) was pretreated under nitrogen from

room temperature to 773 K (3.0 $mL_{SATP}.min^{-1}$) then the gas mixture is introduced at rate of 28.0 $mL_{SATP}.min^{-1}$ (GHSV around 5.6×10^4 h^{-1}). The equations used to calculate conversions of CH_4, CO_2 and yields of H_2, CO are given below [3]:

$$Conversion\ of\ CH_4 = X_{CH_4} = \frac{F_{in(CH_4)} - F_{out(CH_4)}}{F_{in(CH_4)}} \quad (1)$$

$$Conversion\ of\ CO_2 = X_{CO_2} = \frac{F_{in(CO_2)} - F_{out(CO_2)}}{F_{in(CO_2)}} \quad (2)$$

$$Yield\ of\ H_2 = Y_{H_2} = \frac{F_{out(H_2)}}{2\times F_{in(CH_4)}} \quad (3)$$

$$Yield\ of\ CO = Y_{CO} = \frac{F_{out(CO)}}{F_{in(CH_4)} + F_{in(CO_2)}} \quad (4)$$

where F_{in} is the inlet molar flow and F_{out} is the outlet molar flow.

3. Results and Discussion

3.1 Catalysts Characterizations

The BET surface areas and the average pore diameters of the calcined samples are reported in Table 1. It can be seen that for all samples, average pore diameters around 5 nm were obtained indicating a mesoporous texture of our solids. The elaborated samples also revealed very low specific surfaces between 5–7 $m^2.g^{-1}$, which evidences that the partial substitution of nickel by cobalt or copper on both perovskite and spinel structures has no significant effect on the evolution of the BET surface. Indeed, these results are also similar to those reported by Valderrama *et al.* [25], who studied the texture of $LaNiO_3$ and $LaNi_{0.8}Co_{0.2}O_3$ cobalt-type perovskite catalysts, calcined at 1023 K. These authors have measured specific surfaces of the order of 7 $m^2.g^{-1}$ for both catalysts. The nitrogen adsorption-desorption isotherms of the calcined samples, shown in Figure 2-a, are similar to type IV (IUPAC classification [26]) characteristic of mesoporous materials (2–50 nm), which agrees with the obtained pore diameter (around 5 nm). The pore size distribution represented by the BJH curves (Figure 2-b) also confirms the mesoporous character of the elaborated samples with a porous distribution between 2 and 10 nm.

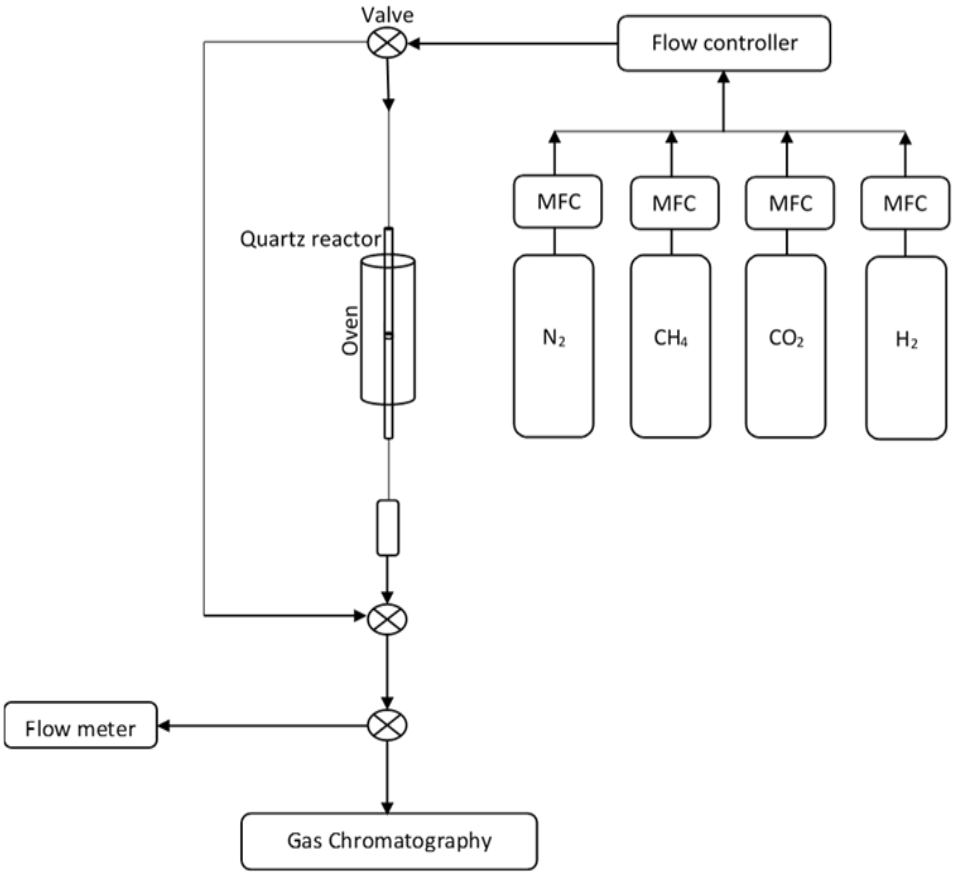

Figure 1. Experimental set up of methane dry reforming.

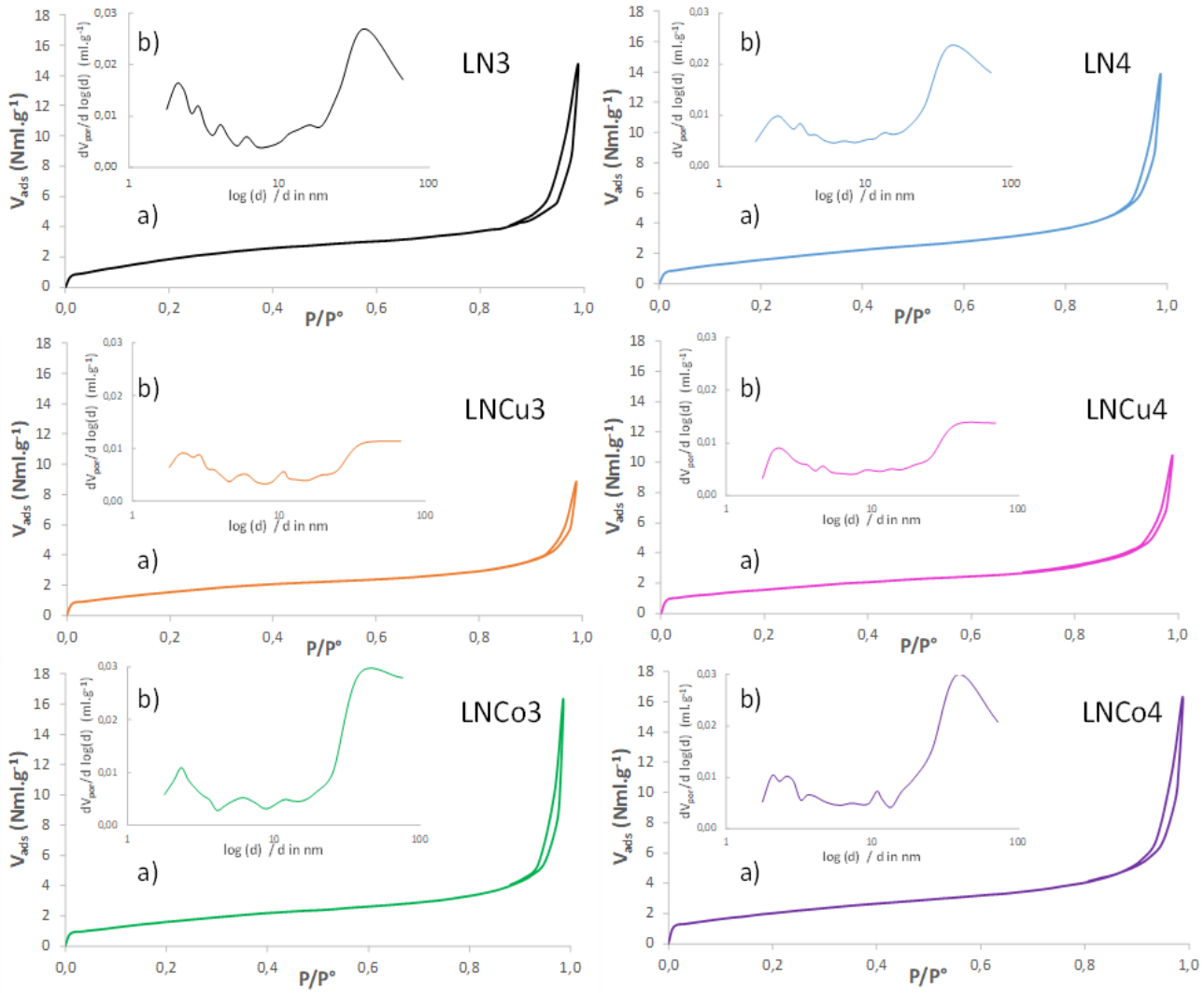

Figure 2. (a) N_2 physisorption isotherms and (b) pore size distribution of the elaborated samples.

Table 1. Specific surface area (S_{BET}), average pore diameter (d_{pore}), experimental H_2 consumption (after H_2-TPR) and reduction degree ($\%_{red}$) of the calcined samples.

Catalyst	S_{BET} ($m^2.g^{-1}$)	d_{pore} (nm)	H_2 $consumption_{exp}$ ($mmol.g^{-1}$)	H_2 $consumption_{theo}$ ($mmol.g^{-1}$)	Reduction degree ($\%_{red}$)
LN3	7.3	4.9	4.04	4.07	99
LN4	5.5	4.3	2.48	2.50	99
LNCo3	6.0	5.7	4.05	4.07	99
LNCu3	5.8	4.8	4.07	4.06	100
LNCo4	7.3	5.7	2.25	2.50	90
LNCu4	5.7	5.4	2.08	2.49	84

Figure 3 shows the XRD patterns of the different fresh catalysts. The diffractogram of non-substituted perovskite $LaNiO_3$ and spinel La_2NiO_4 structures obtained in our previous work [3] are also given as references. As can be seen from the XRD results, the substitution of nickel in perovskite and spinel structures by cobalt or copper affects the crystalline structure. In the case of fresh LNCo3 and LNCu3 samples calcined at 1023 K, the diffractograms reveal the formation of perovskite phases, on the contrary LNCo4 and LNCu4 which present the formation of mixture of spinel phase and lanthanum oxide La_2O_3 (PDF-ICDD 05-0602) with a predominant of La_2O_3 in the case of the cobalt-substituted solid. It is also important to point out that it is difficult to accurately determine the spinel and perovskite phases formed in the case of cobalt-substituted samples. Indeed, an overlap between the diffraction lines of $LaNiO_3$ (PDF-ICDD 33-0711) and $LaCoO_3$ (PDF-ICDD 48-0123) was observed for LNCo3 and between those of La_2NiO_4 (PDF-ICDD 34-0314) and La_2CoO_4 (PDF-ICDD 72-0937) for LNCo4. These overlap phenomena were also observed by G. Valderrama *et al.* when substituting Ni by Co with a substitution ratio ranging from 0 to 1 [25]. On the other hand, the substitution of both perovskite and spinel structures by copper gives rise to the formation of $LaNiO_3$ and La_2NiO_4 phases. No copper based phase was identified. According to the literature, the absence of copper phase or Ni-Cu alloy in the case of Cu-substituted samples can be explained by a good dispersion of copper species in the calcined sample [27–28].

To examine the effect of H_2-reduction on the structure of our materials, samples after H_2-TPR analysis were also characterized by XRD (Figure 4). The diffractograms show the presence of La_2O_3 phase accompanied by the characteristic peaks of metallic nickel Ni^0 (PDF-ICDD 04-0850) for both LNM3 and LNM4 structures. No characteristic peak of metallic cobalt or copper has been detected which may be due to their very low content and /or their good dispersion. We also note the absence of alloy between nickel and cobalt or copper which is confirmed by the H_2-TPR analysis (Figure 5) that highlighted two reduction peaks attribut-

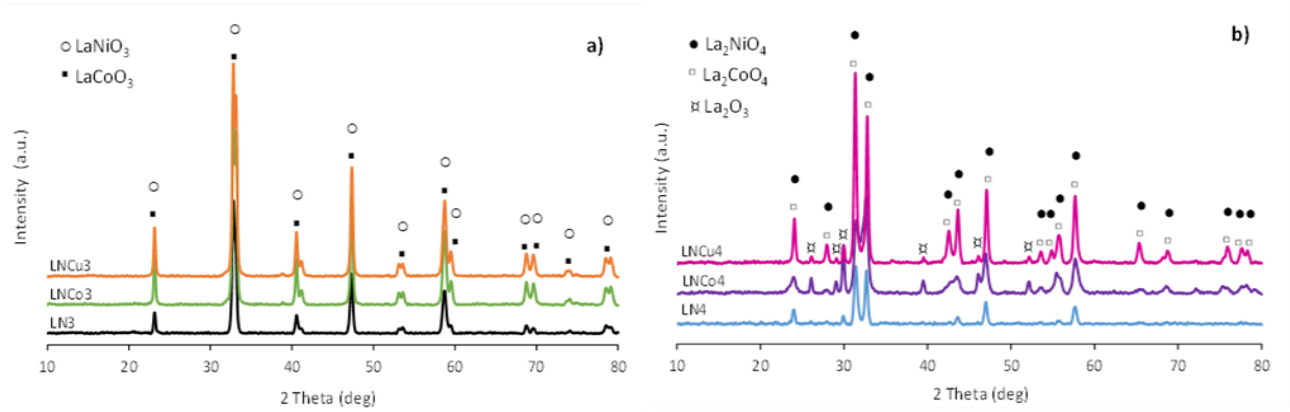

Figure 3. XRD patterns of fresh catalysts: a) LNM3 and b) LNM4 (M = Co, Cu).

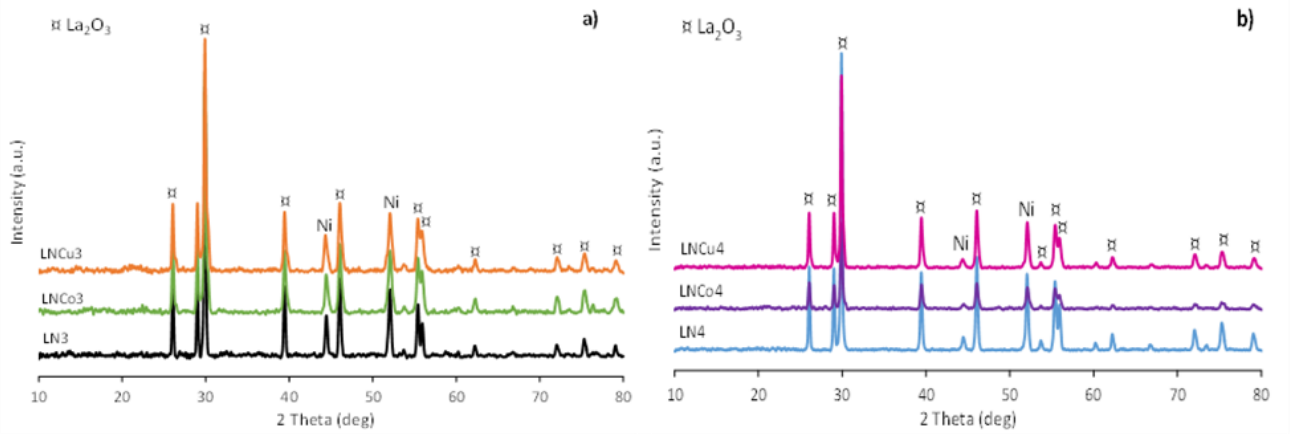

Figure 4. XRD patterns of the samples after H_2-TPR analysis: a) LNM3 and b) LNM4 (M = Co, Cu).

ed to the reduction of Ni^{2+}. Indeed, according to the literature works [26,29], the alloy formation is confirmed by the presence of a single reduction peak indicating that the reduction of bimetallic catalysts (Ni-Co) occurs in one step.

The H_2-TPR profiles of the elaborated LNM3 and LNM4 catalysts are represented in Figure 5. In order to highlight the effect of nickel substitution by cobalt or copper on the reducibility, the profiles of non-substituted spinel La_2NiO_4 and perovskite $LaNiO_3$ samples are also given. For all samples, two reduction peaks are observed. For LNM3 sample, the first one corresponds to the reduction of Ni^{3+} to Ni^{2+} in $La_2Ni_2O_5$ ($2\ LaNiO_3 + H_2 \rightarrow La_2Ni_2O_5 + H_2O$) and also to that of NiO species, while for LNM4 solid, it represents the reduction of NiO to Ni^0. Concerning the second peak, it is attributed to the reduction of Ni^{2+} species present in form of La_2NiO_5 (in LNM3) and La_2NiO_4 (in LNM4) to

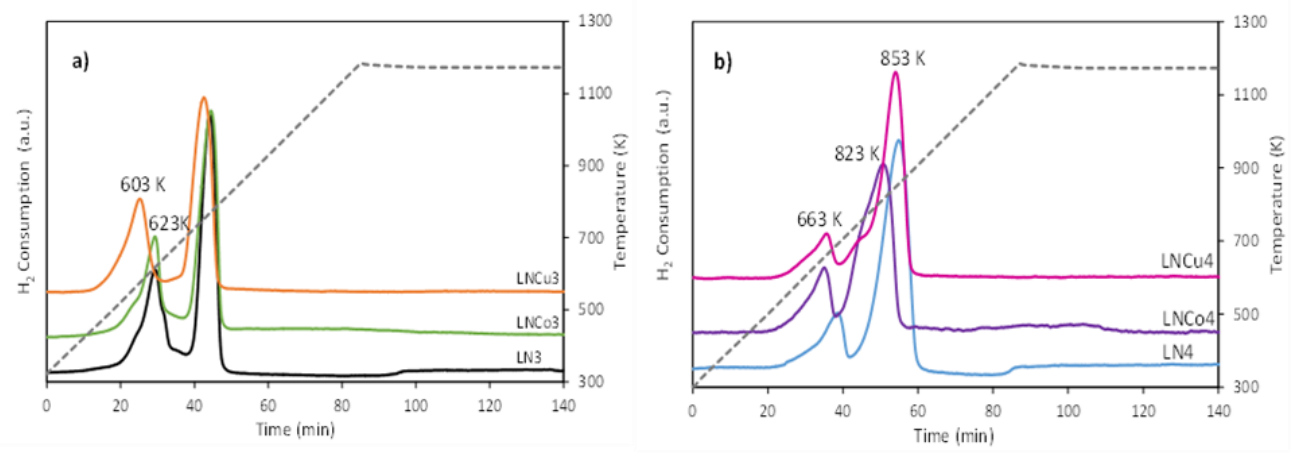

Figure 5. H_2-TPR profiles of fresh catalysts: a) LNM3 and b) LNM4 (M = Co, Cu).

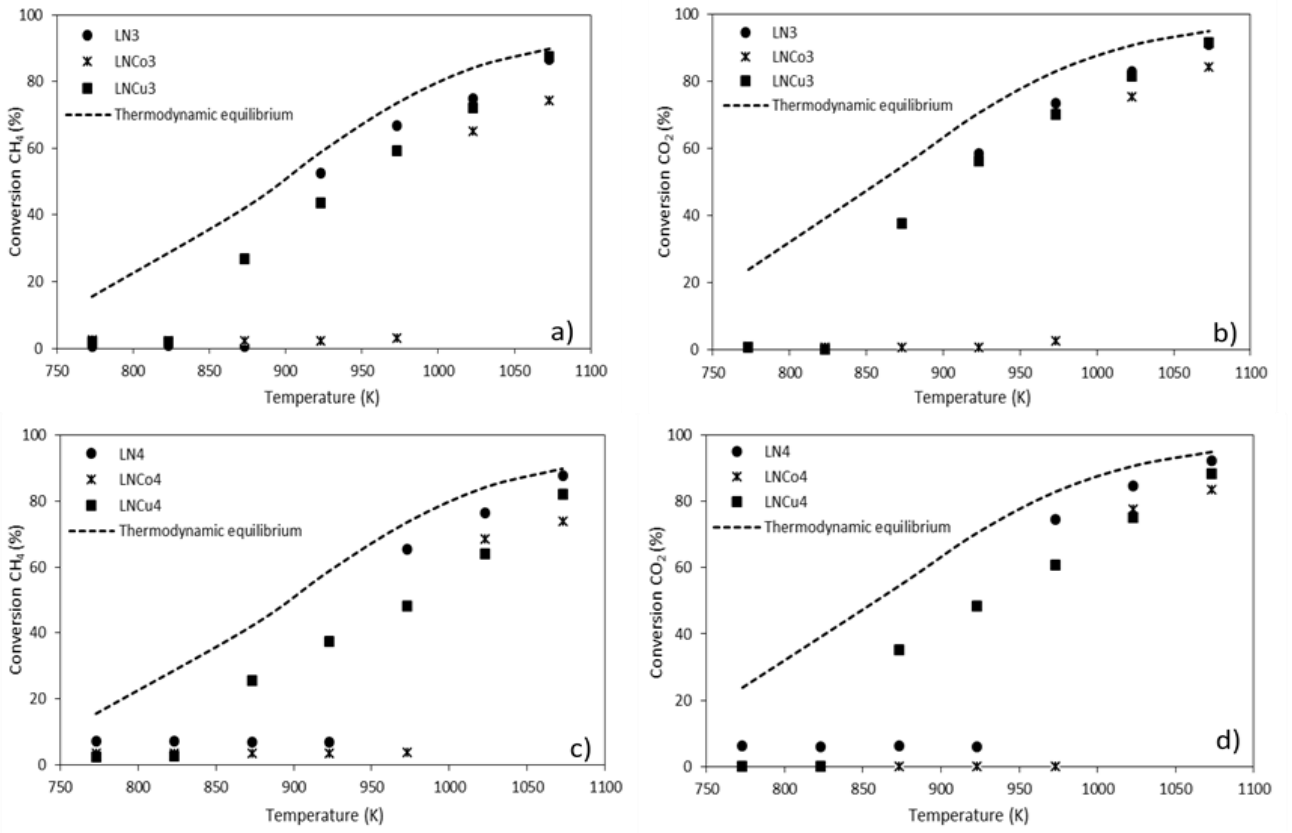

Figure 6. CH_4 (a and c) and CO_2 (b and d) conversions for the prepared catalysts (W/F = 0.0089 g.h.L^{-1}, CH_4/CO_2 = 1.0): LNM3 (a and b) and LNM4 (c and d) (M = Co, Cu). Dotted lines : thermodynamics equilibrium.

lanthanium oxide and metallic nickel as follows: $La_2Ni_2O_5 + 2\ H_2 \rightarrow 2\ Ni + La_2O_3 + 2\ H_2O$ and $La_2NiO_4 + H_2 \rightarrow La_2O_3 + Ni + H_2O$. The LNCo3 profile is similar to that of $LaNiO_3$ perovskite sample. In the case of LNCo4, a 30 K decrease of temperature of both reduction peaks was noted (663 and 823 K for the substituted sample instead of 693 K and 853 K for the La_2NiO_4 oxide). On the contrary, for copper substituted samples, a significant decrease of temperature for the low temperature peak was observed for both structures compare to the non-substituted samples. Indeed, the first reduction peak is observed at 603 K for LNCu3 and at 668 K for LNCu4, which correspond to around 20 K temperature decrease compared to $LaNiO_3$ and 25 K in comparison with La_2NiO_4 respectively. The second peak of reduction was recorded at 768 K for LNCu3 and 853 K for LNCu4 which is close to the temperature of the corresponding non substituted structure. According to Moradi *et al.* [28] and Nataj *et al.* [23], Cu^{2+} is reduced in Cu^0 at temperatures lower than those corresponding to the reduction of Ni^{3+} and Ni^{2+}, and that the presence of Cu^0 crystallites facilitates the reducibilty of nickel cations. The experimental H_2 consumption and reduction degree (%) given in Table 1 indicate that the substituted LNM3 samples are more reducible than LNM4 ones. Indeed, regardless the incorporated metal (Co, Cu), the reduction is almost total in the case of LNM3 while for substituted LNM4 structures, it is estimated at 90% for LNCo4 and 84% for LNCu4.

3.2 Catalysts Reactivity

The reactivity results of LN3, LN4, LNM3, LNM4 (M = Cu or Co) in the dry reforming of methane, obtained in the temperature range (773−1073 K), are presented in Figure 6. Firstly, it can be noted that the nickel substitution by cobalt or copper has a significant effect on the initial conversion temperature of both methane and carbon dioxide. Indeed, the substitution by cobalt delays the activation of CH_4 contrary to copper for which, a decrease in the initial activation temperature (T_{init}) is observed. Comparing the initial activation temperature of both reactants CH_4 and CO_2, the cobalt substituted samples $La_xNi_{0.9}Co_{0.1}O_y$ (x = 1, 2 and y = 3, 4) show an increase of T_{init} (1023 K) com-

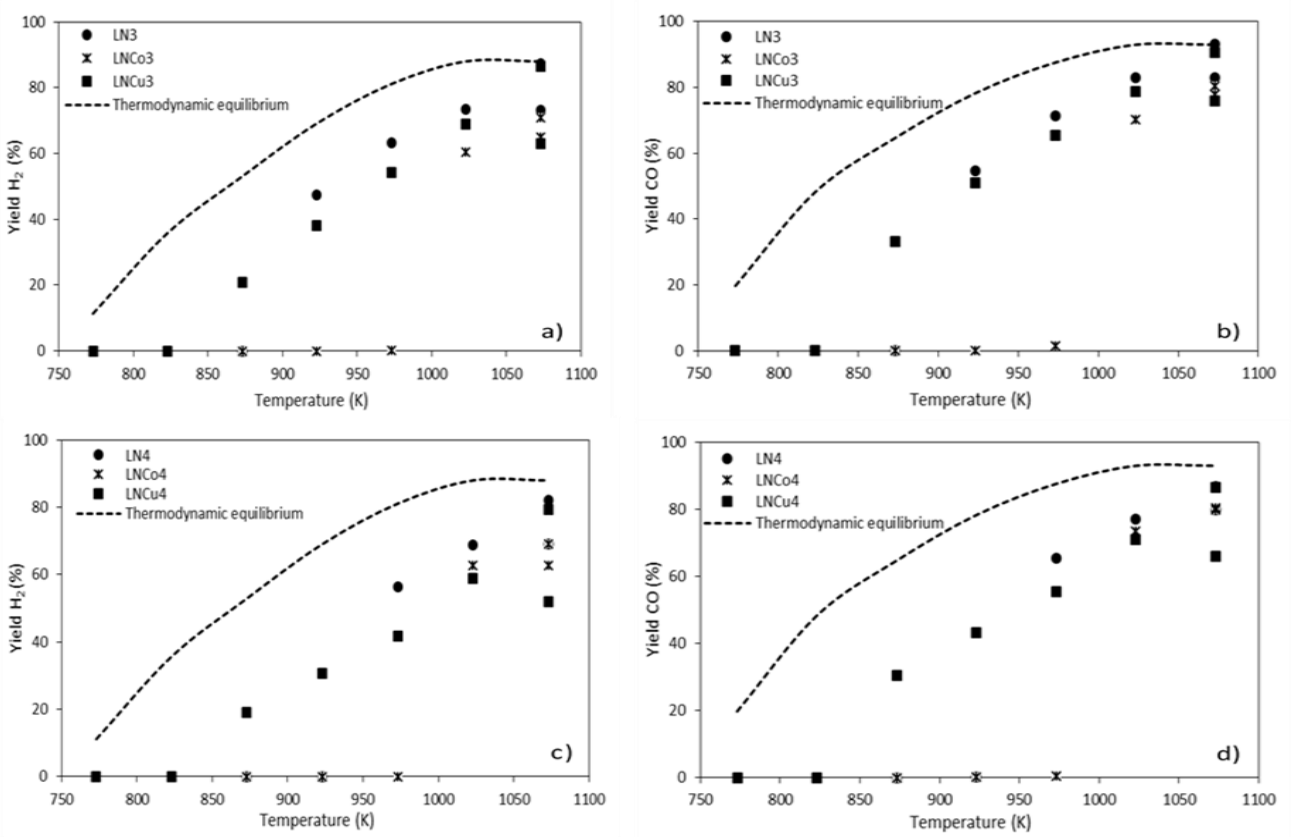

Figure 7: Yields of H_2 (a and c) and CO (b and d) in dry reforming of methane (W/F = 0.0089 g.h.L^{-1}, CH_4/CO_2 = 1): LNM3 (a and b) and LNM4 (c and d) (M = Co, Cu). Dotted lines : thermodynamics equilibrium.

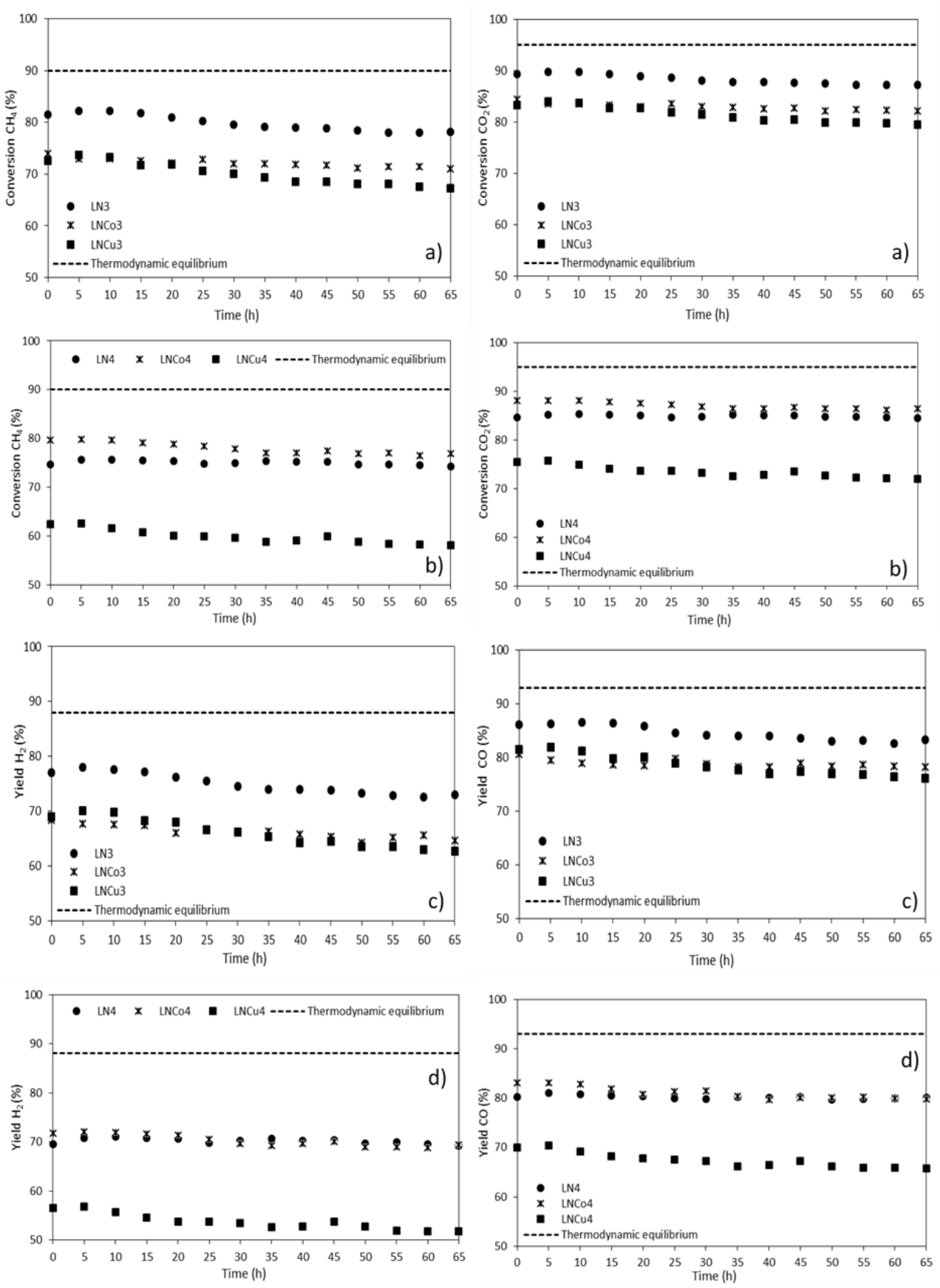

Figure 8. Stability results in DMR of the catalysts prepared by sol-gel method at 1073 K (W/F = 0.0089 g.h.L^{-1}, CH_4/CO_2 = 1): (a) & (c) for LNM3 and (b) & (d) for LNM4 (M = Co, Cu).

pared to the copper substituted catalyst $La_xNi_{0.9}Cu_{0.1}O_y$ (T_{init} = 873 K). At the reaction temperature of 1073 K, the highest CH_4 and CO_2 conversions, estimated respectively at 88 and 91%, are obtained over the copper substituted sample with spinel structure (LNCu4).

The decrease of the activation temperature of both reactants, observed in the case of copper substituted catalysts, can be explained by the formation of Cu^0 crystallites that favors the reducibility of nickel cations to active metallic sites Ni^0. Similar results have been observed by Valderrama *et al.* [25] for $LaCoO_3$ catalyst and Moradi *et al.* [28] in the case of copper substituted catalysts.

The yields of reaction products (CO + H_2) are shown in Figure 7. The measured yields at 1073 K revealed that the copper catalysts LNCu3 and LNCu4 have similar CO and H_2 yields compared to those obtained for corresponding non-substituted LN3 and LN4 samples. No differences were observed between the two structures in the case of copper containing samples (90 and 86% for perovskite LNCu3) and (86 and 79% for spinel LNCu4). However, for the catalysts substituted by cobalt, a significant difference in the product yields is noted for the two structures compared to the non-substituted samples with a higher CO/H_2 ratio at the reactor outlet. This high ratio, indicating an important CO production, suggests the important participation of the reverse water gas (RWGS) reaction for the cobalt based catalysts [31].

The study of the effect of the reaction time on the stability of catalytic performances was carried out at 1073 K during 65 h of catalytic test (Figure 8). Results obtained on non-substituted LN3 and LN4 catalysts show that both catalysts exhibit relatively stable conversions of reactants (76% of CH_4 and 86% of CO_2) and product yields (around 70% of H_2 and 80% of CO) for both samples. However, it is also important to note that the spinel catalyst LN4 is slightly more stable over time than perovskite LN3. This difference in stability may be due to the presence of a larger amount of La_2O_3 in the spinel catalyst, on which CO_2 can adsorb and then migrate in the bulk to form $La_2O_2CO_3$ intermediate; this latter prevents carbon deposition and reduces the deactivation of active nickel species according to the following equation: $La_2O_2CO_3$ + Ni-C → La_2O_3 + 2 CO + Ni [32].

For the substituted catalysts, the obtained stability results show that the cobalt-substituted samples with spinel structure (LNCo4) exhibit the best and most stable conversions (CH_4 and CO_2) and syngas production (H_2 + CO), despite the fact that copper substituted samples activate the methane at lower temperature compared to the Ni-Co catalysts. This better stability of cobalt-substituted catalysts could be explained by a synergistic effect between Ni and Co in the case of nickel-cobalt bimetallic catalysts [25,33–35]. In fact, the coexistence of these two metals contributes to the improvement of the catalytic performances and the stability of the catalysts.

In order to examine the structure evolution and coke deposition, XRD and TPO analyses were carried out on the spent catalysts after 65 h of catalytic test in DRM at 1073 K. The XRD patterns (Figure 9) reveal a total decomposition of the initial phases and the appearance of characteristic peaks of $La_2O_2CO_3$ (PDF-ICDD 048-1113) and Ni^0 in addition to La_2O_3 phase. In fact, as previously mentioned, the formation of the $La_2O_2CO_3$ phase is due to the *in situ* adsorption and bulk migration of CO_2 [36]. Furthermore, no diffraction lines of copper, cobalt or carbon phases were detected for the spent

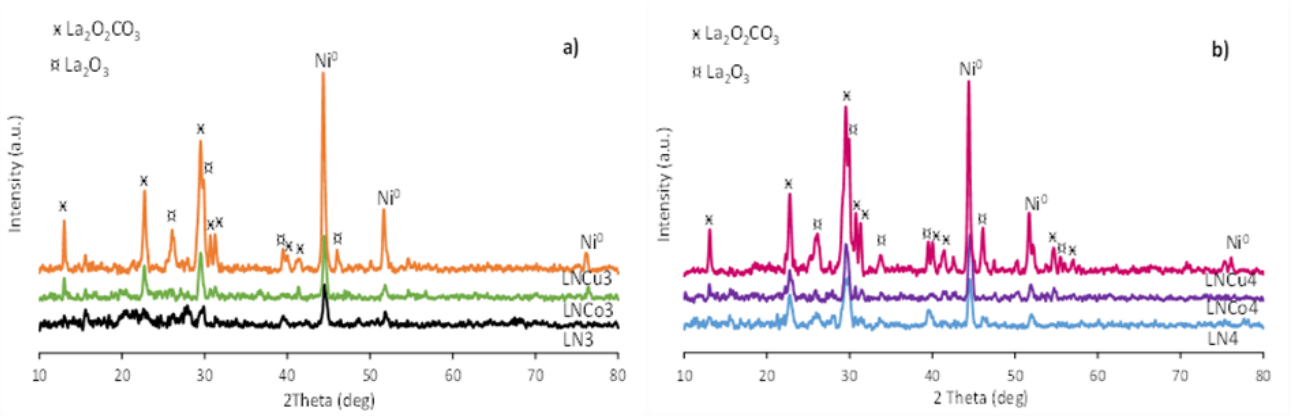

Figure 9: XRD of used catalysts calcined at 1023 K and temperature reaction 1023 K: a) LNM3 and b) LNM4 (M = Co, Cu).

samples, indicating no segregation of copper nor cobalt and no significant formation of structured carbon.

The TPO profiles (Figure 10) giving the oxygen consumption as a function of temperature, show for all the spent catalysts that the oxygen consumption occurred in the temperature range 833−973 K indicating the formation of C_γ-type carbon due to the high reaction temperature and the long reaction time corresponding to nickel carbide NiC and/or carbon nanotubes [37−38].

The Measurements of carbon amounts deposited after 65 h of catalytic test in DRM were performed by TPO analysis. The obtained results reveal that the spinel La_2NiO_4 catalyst leads to low carbon formation (5.6 mmol.g^{-1}) compared to $LaNiO_3$ perovskite (13.3 mmol.g^{-1}), which is in good agreement with the good stability of the La_2NiO_4 sample observed during the DRM reaction. The comparison between the cobalt and copper-substituted solids for the two structures shows that the substitution with cobalt leads to a carbon deposition of 8.2 mmol.g^{-1} in the case of the perovskite LNCo3 and 9.9 mmol.g^{-1} for the spinel LNCo4. On the other hand, the presence of copper in the structure gives rise to amounts of 11.2 and 20.0 mmol.g^{-1} for LNCu3 and LNCu4 respectively. The lower carbon depositions obtained over the Co-substituted catalysts are in good agreement with the reactivity results that have revealed more stable catalytic performances in the case of cobalt samples.

4. Conclusion

The reactivity of $LaNi_{0.9}M_{0.1}O_3$ (LNM3) and $La_2Ni_{0.9}M_{0.1}O_4$ (LNM4) catalysts with M= Co, Cu, prepared by partial substitution of Ni by Co or Cu using sol-gel method, was studied in the dry reforming of methane (DRM) for syngas (CO + H_2) production and their performances were compared to those of $LaNiO_3$ perovskite and La_2NiO_4 spinel. The obtained results highlighted the effect of: (i) the structure type, and (ii) the substitution of nickel by cobalt or copper on the catalytic activity and stability. The reducibility and activity results revealed better catalytic performances in the case of perovskite structure (LN3) due to its high reducibility compared to the spinel one (LN4). The nickel substitution in the $LaNiO_3$ perovskite and La_2NiO_4 spinel structures by cobalt or copper strongly influences the activation temperature of methane and the stability of the catalytic performances over reaction time. The presence of cobalt improves the catalytic stability leading to higher and more stable conversions of CH_4 and CO_2 and syngas (H_2 + CO) production with a low carbon deposition compared to copper samples. These results are strongly related to a synergistic effect between Ni and Co that enhances the catalytic performances in the DRM reaction.

Acknowledgements

The authors would like to thank: Ministère de l'Enseignement Supérieur et de la Recherche Scientifique (MESRS), Alger Algérie for the PNE graduate scholarship that allowed the funding and the achievement of this work.

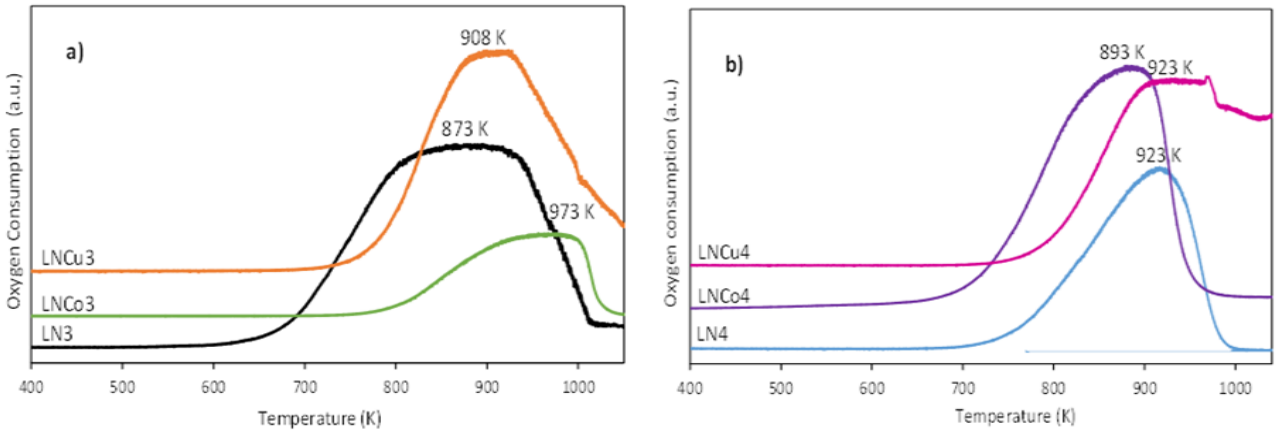

Figure 10. TPO profiles of spent catalysts (after 65 h of catalytic test at 1073 K): a) LNM3 and b) LNM4 (M = Co, Cu).

References

[1] Wood, D.A., Nwaoha, C., Towler, B.F. (2012). Gas-to-liquids (GTL): a review of an industry offering several routes for monetizing natural gas. *J. Nat. Gas. Sci. Eng.*, 9, 196–208. doi: 10.1016/j.jngse.2012.07.001

[2] Iglesias, I., Forti, M., Baronetti, G., Marino, F. (2019). Zr-enhanced stability of ceria based supports for methane steam reforming at severe reaction conditions. *Int. J. Hydrogen Energ.*, 44, 8121–8132. doi: 10.1016/j.ijhydene.2019.02.070

[3] Messaoudi, H., Thomas, S., Djaidja, A., Slyemi, S., Barama, A. (2018). Study of La_xNiO_y and $La_xNiO_y/MgAl_2O_4$ catalysts in dry reforming of methane. *J. CO_2 Util.*, 24, 40–49. doi: 10.1016/j.jcou.2017.12.002

[4] Messaoudi, H., Thomas, S., Djaidja, A., Slyemi, S., Chebout, R., Barama, S., Barama, A., Benaliouche, F. (2017). Hydrogen production over partial oxidation of methane using Ni-Mg-Al spinel catalysts: a kinetic approach. *C.R. Chim.*, 20, 738–746. doi: 10.1016/j.crci.2017.02.002

[5] Zhang, G., Liu, J., Xu, Y., Sun, Y. (2018). A review of CH_4-CO_2 reforming to synthesis gas over Ni-based catalysts in recent years (2010-2017). *Int. J. Hydrogen Energ.*, 43, 15030–15054. doi: 10.1016/j.ijhydene.2018.06.091

[6] Kusakabe, K., Sotowa, K.-I., Eda, T., Iwamoto, Y. (2004). Methane steam reforming over Ce–ZrO_2 supported noble metal catalysts at low temperature. *Fuel Proc. Tech.,* 86, 319–326. doi: 10.1016/j.fuproc.2004.05.003

[7] Profeti, L.P.R., Ticianelli, E.A., Assaf, E.M. (2008). Co/Al_2O_3 catalysts promoted with noble metals for production of hydrogen by methane steam reforming. *Fuel*, 87, 2076–2081. doi: 10.1016/j.fuel.2007.10.015

[8] Swaan, H.M., Kroll, V.C.H., Martin, G.A., Mirodatos, C. (1994). Deactivation of supported nickel catalysts during the reforming of methane by carbon dioxide. *Catal. Today,* 21, 571–578. doi: 10.1016/0920-5861(94)80181-9

[9] Özdemir, H., Öksüzömer, M.A.F., Gürkaynak, M.A. (2010). Preparation and characterization of Ni based catalysts for the catalytic partial oxidation of methane: Effect of support basicity on H_2/CO ratio and carbon deposition. *Int. J. Hydrogen Energ.*, 35, 12147–12160. doi: 10.1016/j.ijhydene.2010.08.091

[10] Al-Fatesh, A.S., Kumar, R., Kasim, S.O., Ibrahim, A.A., Fakeeha, A.H., Abasaeed, A.E., Alrasheed, R., Bagabas, A., Chaudhary, M.L., Frusteri, F., Chowdhury, B. (2020). The effect of modifier identity on the performance of Ni-based catalyst supported on γ-Al_2O_3 in dry reforming of methane. *Catal. Today,* 348, 236–242. doi: 10.1016/j.cattod.2019.09.003

[11] Wang, F., Wang, Y., Zhang, L., Zhu, J., Han, B., Fan, W., Xu, L., Yu, H., Cai, W., Li, Z., Deng, Z., Shi, W. (2020). Performance enhancement of methane dry reforming reaction for syngas production over $Ir/Ce_{0.9}La_{0.1}O_2$-nanorods catalysts. *Catal. Today,* 355, 502–511. doi: 10.1016/j.cattod.2019.06.067

[12] Benrabaa, R., Barama, A., Boukhlouf, H., Guerrero-Caballero, J., Rubbens, A., Bordes-Richard, E., Löfberg, A., Vannier, R.N. (2017). Physico-chemical properties and syngas production via dry reforming of methane over $NiAl_2O_4$ catalyst. *Int. J. Hydrogen Energ.*, 42, 12989–12996. doi: 10.1016/j.ijhydene.2017.04.030

[13] Dama, S., Ghodke, S.R., Bobade, R., Gurav, H.R., Chilukuri, S. (2018). Active and durable alkaline earth metal substituted perovskite catalysts for dry reforming of methane. *Appl. Catal. B: Environ.,* 224, 146–158. doi: 10.1016/j.apcatb.2017.10.048

[14] Song, X., Dong, X., Yin, S., Wang, M., Li, M., Wang, H. (2016). Effects of Fe partial substitution of $La_2NiO_4/LaNiO_3$ catalyst precursors prepared by wet impregnation method for the dry reforming of methane. *Appl. Catal. A: Gen.*, 526, 132–138. doi: 10.1016/j.apcata.2016.07.024

[15] Guo, J., Lou, H., Zhao, H., Chai, D., Zheng, X. (2004). Dry reforming of methane over nickel catalysts supported on magnesium aluminate spinels. *Appl. Catal. A: Gen.*, 273, 75–82. doi: 10.1016/j.apcata.2004.06.014

[16] Li, Z., Li, M., Bian, Z., Kathiraser, Y., Kawi, S. (2016). Design of highly stable and selective core/yolk–shell nanocatalysts-A review. *Appl. Catal. B: Environ.*, 188, 324–341. doi: 10.1016/j.apcatb.2016.01.067

[17] Peng, H., Zhang, X., Zhang, L., Rao, C., Lian, J., Liu, W., Ying, J., Zhang, G., Wang, Z., Zhang, N., Wang, X. (2017). One-Pot Facile Fabrication of Multiple Nickel Nanoparticles Confined in Microporous Silica Giving a Multiple-Cores@Shell Structure as a Highly Efficient Catalyst for Methane Dry Reforming. *ChemCatChem.*, 9, 127–136. doi: 10.1002/cctc.201601263

[18] Dai, C., Zhang, S., Zhang, A., Song, C., Shi, C., Guo, X. (2015). Hollow zeolite encapsulated Ni–Pt bimetals for sintering and coking resistant dry reforming of methane. *J. Mater. Chem. A,* 3, 16461–16468. doi: 10.1039/C5TA03565A

[19] Zhu, Y., Jin, N., Liu, R., Sun, X., Bai, L., Tian, H., Ma, X., Wang, X. (2020). Bimetallic $BaFe_2MAl_9O_{19}$ (M = Mn, Ni, and Co) hexaaluminates as oxygen carriers for chemical loop-

ing dry reforming of methane. *Appl. Energy,* 258, 114070–114074. doi: 10.1016/j.apenergy.2019.114070

[20] Horlyck, J., Lawrey, C., Lovell, E.C., Amal, R., Scott, J. (2018). Elucidating the impact of Ni and Co loading on the selectivity of bimetallic NiCo catalysts for dry reforming of methane. *Chem. Eng. J.*, 352, 572–580. doi: 10.1016/j.cej.2018.07.009

[21] Song, K., Lu, M., Xu, S., Chen, C., Zhan, Y., Li, D., Au, C., Jiang, L., Tomishige, K. (2018). Effect of alloy composition on catalytic performance and coke-resistance property of Ni-Cu/Mg(Al)O catalysts for dry reforming of methane. *Appl. Catal. B: Environ.*, 239, 324–333. doi: 10.1016/j.apcatb.2018.08.023

[22] Fan, M.S., Abdullah, A.Z., Bhatia, S. (2010). Utilization of greenhouse gases through carbon dioxide reforming of methane over Ni–Co/MgO–ZrO_2: Preparation, characterization and activity studies. *Appl. Catal. B: Environ.*, 100, 365–377. doi: 10.1016/j.apcatb.2010.08.013

[23] Nataj, S.M.M., Alavi, S.M., Mazloom, G. (2018). Modeling and optimization of methane dry reforming over Ni-Cu/Al_2O_3 catalyst using Box-Behnken design. *J. Energy Chem.*, 27, 1475–1488. doi: 10.1016/j.jechem.2017.10.002

[24] Shiri, A., Soleymanpour, F., Eshghi, H., Khosravi, I. (2015). Nano-sized $NiLa_2O_4$ spinel–$NaBH_4$-mediated reduction of imines to secondary amines. *Chin. J. Catal.*, 36, 1191–1196. doi: 10.1016/S1872-2067(15)60921-4

[25] Valderrama, G., Kiennemann, A., Goldwasser, M.R. (2008). Dry reforming of CH_4 over solid solutions of $LaNi_{1-x}Co_xO_3$. *Catal. Today,* 133–135, 142–148. doi: 10.1016/j.cattod.2007.12.069

[26] Leofanti, G., Padovan, M., Tozzola, G., Venturelli, B. (1998). Surface area and pore texture of catalysts. *Catal. Today,* 41, 207–219. doi: 10.1016/S0920-5861(98)00050-9

[27] Valderrama, G., Kiennemann, A., Goldwasser, M.R. (2010). La-Sr-Ni-Co-O based perovskite-type solid solutions as catalyst precursors in the CO_2 reforming of methane. *J. Power Sources,* 195, 1765–1771. doi: 10.1016/j.jpowsour.2009.10.004

[28] Moradi, G.R., Khosravian, F., Rahmanzadeh, M. (2012). Effects of Partial Substitution of Ni by Cu in $LaNiO_3$ Perovskite Catalyst for Dry Methane Reforming. *Chinese J. Catal.,* 33, 797–801.doi: 10.1016/S1872-2067(11)60378-1

[29] Banerjee, A., Das, S., Mirsa, S., Mukhopadhyay, S. (2009). Structural analysis on spinel ($MgAl_2O_4$) for application in spinel-bonded castables. *Ceramics Int.,* 35, 381–390. doi: 10.1016/j.ceramint.2007.11.009

[30] Guo, J., Lou, H., Zhao, H., Wang, X. (2004). Novel synthesis of high surface area $MgAl_2O_4$ spinel as catalyst support. *Mat. Let.,* 58, 1920–1923. doi: 10.1016/j.matlet.2003.12.013

[31] Phan, T.S., Sane, A.R., de Vasconcelos, B.R., Nzihou, A., Sharrock, P., Grouset, D., Pham Minh, D. (2018). Hydroxyapatite supported bimetallic cobalt and nickel catalysts for syngas production from dry reforming of methane. *Appl. Catal. B: Environ.*, 224, 310–321. doi: 10.1016/j.apcatb.2017.10.063

[32] Verykios, X.E. (2003). Catalytic dry reforming of natural gas for the production of chemicals and hydrogen. *Int. J. Hydrogen Energ.,* 28, 1045–1063. doi: 10.1016/S0360-3199(02)00215-X

[33] Zhang, J., Wang, H., Dalai, A.K. (2007). Development of stable bimetallic catalysts for carbon dioxide reforming of methane. *J. Catal.*, 249, 300–310. doi: 10.1016/j.jcat.2007.05.004

[34] Takanabe, K., Nagaoka, K., Nariai, K., Aika, K. (2005). Titania-supported cobalt and nickel bimetallic catalysts for carbon dioxide reforming of methane. *J. Catal.,* 232, 268–275. doi: 10.1016/j.jcat.2005.03.011

[35] González, O., Lujano, J., Pietri, E., Goldwasser, M.R. (2005). New Co-Ni catalyst systems used for methane dry reforming based on supported catalysts over an INT-MM1 mesoporous material and a perovskite-like oxide precursor $LaCo_{0.4}Ni_{0.6}O_3$. *Catal. Today,* 107–108, 436–443. doi: 10.1016/j.cattod.2005.07.112

[36] Song, X., Dong, X., Yin, S., Wang, M., Li, M., Wang, H. (2016). Effects of Fe partial substitution of $La_2NiO_4/LaNiO_3$ catalyst precursors prepared by wet impregnation method for the dry reforming of methane. *Appl. Catal. A: Gen.*, 526, 132–138. doi: 10.1016/j.apcata.2016.07.024

[37] Djaidja, A., Libs, S., Kiennemann, A., Barama, A. (2006). Characterization and activity in dry reforming of methane on NiMg/Al and Ni/MgO catalysts. *Catal. Today,* 113, 194–200. doi: 10.1016/j.cattod.2005.11.066

[38] Djaidja, A., Messaoudi, H., Kaddeche, D., Barama, A. (2015). Study of Ni-M/MgO and Ni-M-Mg/Al (M= Fe or Cu) catalysts in the CH_4-CO_2 and CH_4-H_2O reforming. *Int. J. Hydrogen Energ.,* 40, 4989–4995. doi: 10.1016/j.ijhydene.2014.12.106